

# 1 The flexural strength of bonded ice

2 Andrii Murdza<sup>1</sup>, Arttu Polojärvi<sup>2</sup>, Erland M. Schulson<sup>1</sup>, Carl E. Renshaw<sup>1,3</sup>

3 <sup>1</sup>Thayer School of Engineering, Dartmouth College, Hanover, NH, USA

4 <sup>2</sup>Aalto University, School of Engineering, Department of Mechanical Engineering, P.O. Box 14100, 00076 Aalto,  
5 Finland

6 <sup>3</sup>Department of Earth Sciences, Dartmouth College, Hanover, NH, USA

7 *Correspondence to:* Andrii Murdza (Andrii.Murdza@dartmouth.edu)

8 **Abstract.** The flexural strength of ice surfaces bonded by freezing, termed freeze-bond, was studied by performing  
9 four-point-bending tests of bonded freshwater S2 columnar-grained ice samples in the laboratory. The samples were  
10 prepared by milling the surfaces of two ice pieces, wetting two of the surfaces with water of varying salinity, bringing  
11 these surfaces together, and then letting them freeze under a compressive stress of about 4 kPa. The salinity of the  
12 water used for wetting the surfaces to generate the bond varied from 0 to 35 ppt. Freezing occurred in air under  
13 temperatures varying from -25 to -3 °C over periods that varied from 0.5 h to ~100 hours. Results show that an increase  
14 in bond salinity or temperature leads to a decrease in bond strength. The trend for the bond strength as a function of  
15 salinity is similar to that presented in Timco and O'Brien (1994) for saline ice. No freezing occurs at -3 °C once the  
16 salinity of the water used to generate the bond exceeds ~25 ppt. The strength of the saline ice bonds levels off (i.e.,  
17 saturates) within 6-12 hours of freezing; bonds formed from fresh water reach strengths that are comparable or higher  
18 than that of the parent material in less than 0.5 hours.

## 19 1. Introduction

20 Freeze bonds form when distinct ice features, such as floating ice floes or ice blocks of a rubble pile, become  
21 and remain in contact over a period of time at low enough temperature. Insight into the strength of the bonds is  
22 important when, for example, the strength of an ice cover formed of refrozen floes or the strength of an ice rubble pile  
23 is estimated. There are several factors that affect the failure of a cover of sea ice, surface waves being a major one  
24 that has gained an increasing amount of interest recently (Shen, 2017; Squire, 2020). Under the action of waves, ice  
25 covers bend and may undergo flexural failure (Arduin et al., 2020; Asplin et al., 2012; Collins et al., 2015; Hwang  
26 et al., 2017; Kohout et al., 2014, 2016; Shackleton, 1982). It is relevant to ask if the freeze bonds forming into vertical  
27 cracks within a broken and refrozen ice cover form the weakest link at which wave-induced cracks initiate and  
28 propagate. During the wave-ice interaction, the freeze bonds deform and failure occurs under a tensile state of stress  
29 arising from flexural deformation. Szabo and Schneebeli (2007) performed tensile tests on sintered ice grains on scale  
30  $\sim 10^{-3}$  m, but to our knowledge, no data on freeze-bond strength under tensile loading at time and length scales relevant  
31 to geophysical or ice engineering problems have been published.

33 The strength of freeze bonds has been tested only under combined compressive and shear loading. Such tests  
34 have been related to continuum modeling of ice rubble using material models having yield surfaces resembling that  
35 of a Mohr-Coulomb material model (Ettema and Urroz, 1989; Heinonen, 2004; Liferov et al., 2002, 2003; Serré,  
36 2011b, 2011a). The critical shear stress of a Mohr-Coulomb material is given by  $\tau = c + \sigma \tan \varphi$ , where  $c$  is the  
37 cohesion,  $\sigma$  the compressive stress, and  $\varphi$  the internal friction angle of the material. The underlying assumption in  
38 testing has been that the failure of the individual freeze bonds within the rubble occurs through the same mode as the  
39 failure of the rubble itself. No evidence of this type of similarity between the two scales exists. Instead, the numerical  
40 simulations (Polojärvi and Tuhkuri, 2013) suggest that the individual freeze bonds within deforming rubble do not  
41 fail due to shear, but rather under tensile stresses as the bonded ice blocks move relative to each other. This implies  
42 that data on the shear strength of the freeze bonds may not lead to reliable estimates of the shear strength of ice rubble.  
43

44 In this paper, the strength of freeze bonds under tensile loading is studied. For this purpose, we conducted  
45 four-point-bending tests using the apparatus described and used by Murzda et al. (2020). All procedures for testing  
46 were designed with the aim of reducing the number of variables for reliable analysis: bonds were formed between  
47 milled surfaces of freshwater ice specimens (termed the parent material) and bond freezing and testing were performed  
48 in air under a small compressive stress of about 4 kPa. The experimental variables were the freezing time (0.5 h...~100  
49 h), the sample temperature (-3°C...-25°C), and the salinity of the water used to form the bond (0...35 ppt). Bond  
50 strength initially increases with freezing time, but then appears to level off and to reach a plateau (i.e., to saturate)  
51 over several hours. Depending on the salinity of the water from which the bond is formed, the saturation time for bond  
52 strength ranges from 0.5 h to 12 h. The “saturated strength” of freshwater bonds with finer microstructure appears to  
53 reach levels higher than the strength of the parent material with a larger grain size. The results from these experiments,  
54 presented below, represent the first set of results on the failure of freeze bonds under tension.

## 55 2. Experimental procedure

56 Freshwater ice, used here as the parent material for the freeze-bonded samples, was produced in the  
57 laboratory as described in Smith and Schulson (1993) and Golding and others (2010). Tap-water was frozen  
58 unidirectionally from top to bottom in a cylindrical 800 L polycarbonate tank, forming pucks of ~1 m in diameter and  
59 ~25 cm in thickness. The ice was generally bubble-free and columnar-grained. Thin-section analysis showed that the  
60 average column diameter, as measured in the horizontal plane normal to the direction of ice growth using the linear  
61 intercept method, was  $5.5 \pm 1.3$  mm. The c-axes were randomly oriented within, and confined to, the horizontal plane,  
62 suggesting that the ice had an S2 growth texture (in the terminology of Michel and Ramseier, 1971). The ice density  
63 was  $914.1 \pm 1.6$  kg·m<sup>-3</sup> (Golding and others, 2010); Young’s modulus in the horizontal plane was 9.52 GPa (Snyder  
64 and others, 2016). Once grown, the ice was cut into blocks and stored in plastic cooler boxes in a cold room at -10° C.  
65 Specimen preparation is described in detail elsewhere (Iliescu et al., 2017; Murzda et al., 2018, 2019, 2020c, 2020a).  
66

67 Samples to be freeze-bonded were prepared from the ice blocks by milling them into thin plates. The plates  
68 had dimensions of  $h \sim 15$  mm in thickness (parallel to the long axis of the grains),  $b \sim 85$  mm in width, and  $l \sim 300$  mm  
69 in length. Specimens were allowed to equilibrate to the test temperature for at least 24 hours prior to testing.

70  
71 The plates were then cut perpendicular to their long axis into two parts. In most samples the sawn surfaces  
72 were milled after cutting (more below). The two parts of the specimen were then placed in a cold room with a  
73 temperature of  $+2^\circ\text{C}$  for a few minutes. To initiate freeze-bond growth, the sawn and milled surfaces were sprayed  
74 with a fine mist of water at a temperature of  $+2^\circ\text{C}$  and quickly brought into contact by setting the two pieces into a  
75 freeze-bonding rig (Figure 1). The surfaces were wet when brought into contact, but in addition, a syringe was used  
76 to inject about 0.1 ml of water to the bond to ensure uniform wetting of the surfaces. Excess water, if any was observed  
77 around the bond, was wiped with a tissue. All of the above steps were performed at  $+2^\circ\text{C}$  to prevent freezing from  
78 occurring before setting the sample into the rig. Afterwards, the freeze-bonding rig was moved to another cold room  
79 with a desired test temperature.

80  
81 To investigate whether the roughness of the faces in contact affects the bond strength, a few samples had  
82 their faces produced by cutting the parent plate either with a coarse (1/2 inch in width, 1/40 inch in thickness and  
83 6 teeth per inch) or a fine (13/64 inch in width, 1/64 inch in thickness and 24 teeth per inch) band saw. Although few  
84 in number, results from these initial experiments suggested that surface roughness of the kind we explored had no  
85 significant effect on flexural strength. Thus, for all further tests (that led to the results reported below) sawn surfaces  
86 were milled for consistency and reproducibility (more in Discussion).

87  
88 Figure 1 shows a sketch (a) and photograph (b) of the freeze-bonding rig. The rig had a system consisting of  
89 two plastic bars and two springs for applying a desired pressure (i.e., compressive stress) to the bond during freezing.  
90 In the present experiments, a confining pressure of  $\sim 4$  kPa was chosen which is in accordance with the maximum  
91 hydrostatic pressure within submerged 10-meter-thick ice rubble mass (Ettema and Schaefer, 1986). The rig was kept  
92 in a cold room of the desired temperature (i.e. from  $-25^\circ\text{C}$  to  $-3^\circ\text{C}$ ) during freezing. The base of the rig was made from  
93 an acrylic plate having low heat conductivity, ensuring the heat flux in the bond area was mainly along the long axis  
94 of the sample. Wax paper was placed between the ice and the acrylic to prevent freezing of ice onto the rig. All  
95 materials of the rig were such that the frictional resistance between them and ice was low. This enabled good control  
96 of the confining pressure and sample alignment.

97  
98 To investigate the effect of the salinity on the bond strength, fresh water and saline water of salinity ranging  
99 from 2 to 35 ppt (parts per thousand), was used in spraying. Saline water was prepared in the manner described by  
100 Golding et al. (2010, 2014) by adding the commercially available salt mixture "Instant Ocean" to tap water. Salinity  
101 was measured using a calibrated YSI Pro30 conductivity salinity meter.

102

103 After a desired time of freezing, varying from 0.5 to ~100 h, the freeze-bonded sample was removed from  
104 the rig and its flexural strength under four-point bending was measured. For this purpose, a servo-hydraulic loading  
105 system (MTS model 810.14) with a custom-built four-point loading frame was utilized. The sketch of the apparatus  
106 is shown in Figure 2 of Murdza et al. (2020c), the photograph of the apparatus is shown in Figure 5a and the apparatus  
107 is described in detail elsewhere (Iliescu et al., 2017; Murdza et al., 2018, 2019, 2020c). The outer loading rollers are  
108 immobile during testing while the inner loading rollers are attached to the actuator. The hydraulic actuator was driven  
109 under displacement control and loading was controlled using a FlexTest-40 controller. A calibrated load cell was used  
110 to measure the load.

111  
112 The experiments were performed at an outer-fiber center-point displacement rate of  $0.1 \text{ mm s}^{-1}$  (or outer-  
113 fiber strain rate of about  $1.4 \times 10^{-4} \text{ s}^{-1}$  according to linear-elastic first order beam theory). This displacement rate  
114 resulted in an outer-fiber stress rate of about  $1 \text{ MPa s}^{-1}$ . As was indicated earlier (Murdza et al., 2020c), the  $0.1 \text{ mm s}^{-1}$   
115 displacement rate in cycling results in a period of ~20 s which is approximately the frequency of ocean swells (Collins  
116 and others, 2015). The major outer-fiber stress  $\sigma_f$  was calculated as:

$$\sigma_f = \frac{3PL}{4bh^2}, \quad (1)$$

117 where  $P$  is the applied load and  $L$  is the distance between the outer pair of loading cylinders and is set by the geometry  
118 of the apparatus to be  $L = 254 \text{ mm}$ . The flexural strength that we refer to throughout this paper is the maximum major  
119 outer-fiber stress that the ice plate can withstand before breaking (assuming the material is linear-elastic and brittle).  
120 It is important to note that in all experiments described in this paper the bond formation and breaking of bonded ice  
121 occurred at the same temperature. Owing to the confining impact of the loading cylinders of the 4-point flexing  
122 apparatus (see Figure 5a and Figure 2 of Murdza et al. (2020c)) and to the Poisson effect, a biaxial state of tension  
123 developed in the ice. ~~Based on isotropic elasticity and plasticity theories, the minor stress was approximately between~~  
124 ~~one-third to one-half of the major stress (Appendix A).~~

### 125 3. Results and Observations

#### 126 3.1. Flexural strength of parent material

127 Two measurements on the flexural strength of pristine ice plates, that is, plate-like samples of parent material  
128 without a freeze bond, were conducted at  $-10 \text{ }^\circ\text{C}$ . The strength values obtained were 1.51 and 1.63 MPa. Only two  
129 experiments were performed as these values compare favorably with the earlier measurements (Murdza et al., 2020c)  
130 on the same kind of ice using the same loading system. Murdza et al. (2020c) reported that the average and the standard  
131 deviation of the flexural strength at  $-3$ ,  $-10$  and  $-25 \text{ }^\circ\text{C}$  were  $1.42 \pm 0.16$ ,  $1.67 \pm 0.22$  and  $1.89 \pm 0.01 \text{ MPa}$ , respectively.  
132 Further, the measured values are in agreement with the data that are reviewed in Timco and O'Brien (1994), where  
133 the average and standard deviation of  $1.73 \pm 0.25 \text{ MPa}$  is reported for the flexural strength of freshwater ice at  
134 temperatures below  $-4.5 \text{ }^\circ\text{C}$ .

135 **3.2. Flexural strength of bonded ice**

136 **3.2.1. Freshwater bond**

137 The experiments with a freshwater bond were conducted at -3 and -10 °C. The results are listed in Table 1.  
138 The shortest time of 0.5 hours used here for the bond formation implies that the bond formed in less time. (0.5 hours  
139 was the shortest freezing period used here, implying that the bond formed in less time) is reasonably consistent with  
140 analytical estimates, Appendix B. Surprisingly, in all of these experiments, the failure occurred outside of the bond.  
141 This suggests that even after only a relatively short period of freezing, the strength of the freshwater bond reaches and  
142 exceeds that of the parent material. Even though the results listed in Table 1 show scatter, at -10°C comparison of the  
143 measured flexural strengths to those described in Section 3.1 showed that they are not statistically different from the  
144 flexural strength of pristine freshwater ice samples (*p-value* = 0.21 and 0.08 for tests at -3 and -10 °C, respectively).  
145 This is important because it indicates that the above-described bond generation procedure did not hamper the samples  
146 by, for example, leading to geometrical misalignments in them.

147 **3.2.2. Saline bond**

148 Figures 2 and 3 show the results from the experiments performed to investigate the effect on bond strength  
149 of the salinity of the water used to create the freeze bond. The data are given in Tables 2-4. The tables indicate the  
150 experiments where no freezing occurred (“No”) and the experiments where bonding occurred, but the bond was too  
151 weak to be tested (“Low”). These data are excluded in the figures below.

152  
153 Figure 2 shows that the strength of the saline bonds increases over time and levels off, or saturates, after  
154 about 6-12 h. Thus, the strength of the saline bonds increases at a considerably lower rate than that of the freshwater  
155 bonds. A comparison of these results to those in Section 3.1 shows that the strength of the saline bonds is well below  
156 the strength of the freshwater ice used as the parent material. A comparison of the two data sets in Figure 2 shows  
157 that the saturated strength of the bonds made from water of higher salinity but at lower temperature (35 ppt and -  
158 10 °C) is about twice of that of the bonds with lower salinity but higher temperature (12 ppt and -3 °C).

159 Figure 3 illustrates how the salinity of the water used to generate the freeze-bond at -3 °C affects its saturated  
160 strength at -3 °C. While the measured strength values for low salinities are close to those measured for freshwater ice,  
161 the bond strength decreases rapidly with an increase in salinity and no freezing occurs once the salinity of the salt  
162 water used to generate the bond reaches ~25 ppt; even at 17 ppt some bonds were too weak to be tested. This agrees  
163 reasonably well with analytical estimates, Appendix EA, where formulas that relate strength to volume fraction of  
164 solid phase suggest that at salinities of 30 ppt and above at -3 °C no freezing occurs. Figure 3 additionally shows two  
165 exponential fits, one directly fitted to our data and one by Timco and O’Brien (1994) for the flexural strength of saline  
166 ice (equations for these fits provided in Appendix EB, where  $\sigma_b$  is flexural strength in MPa and  $v_b$  is liquid brine  
167 content in parts per thousand). It is important to notice that the fit by Timco and O’Brien (1994) yields lower values  
168 than the measured bond strength in the present study for the whole range of salinities used. Likewise, the actual  
169 strength values for the freshwater bonds are greater than the ones suggested by Figure 3, since the failure in these

Field Code Changed

Formatted: Not Highlight

Formatted: Not Highlight

Formatted: Not Highlight

Formatted: Not Highlight

170 cases occurred outside the bond, indicating that the bond is stronger than the parent material. Both saline and  
171 freshwater bonds that develop through freezing appear to reach strengths higher than that of S2 type parent material  
172 of the same salinity (strength of saline parent material is assumed to be the same as in Timco and O'Brien (1994)).

173 Temperature has a strong effect on the saturated strength of the freeze bonds. Figure 4 and Table 5 summarize  
174 the data from experiments on specimens having bonds made from water of salinity 20 ppt at temperatures from -3 °C  
175 to -25 °C. Three out of the four specimens at -25 °C failed outside of the bond with a measured strength of  
176  $1.61 \pm 0.12$  MPa, which is close to 1.89 MPa measured earlier at -25 °C on the same type of freshwater ice (Murdza et  
177 al., 2020c). Figure 4 also suggests that no freezing occurs at temperatures above about -3 °C, which is in fair agreement  
178 with analytical estimates of no strength at  $T = -2$  °C in Appendix [E.A](#). Though the analytical equation from Appendix [E](#)  
179 [A](#) predicts well when no freezing occurs, it does not yield a trend that describes most of the data in Figure 4. The  
180 reason may be that for the microstructure of bonds in the present study, strength may not be directly proportional to  
181 volume fraction of the solid phase as the model in Appendix [E.A](#) assumes, but rather a non-linear function of the  
182 volume fraction of solid.

183 Figure 5a-c show an example of the typical samples after failure. Figure 5a shows a case where the crack had  
184 initiated at the bond and started to propagate along it, but then deviated from it and continued to grow through the  
185 parent material. Figure 5b shows a close up of a bond face-on after the most common type of failure, which occurred  
186 along the bond. In this case, both surfaces of the failed freeze-bond had a fairly uniform “blurry” appearance which  
187 indicates that failure occurred through the ice of the bond. It was also fairly usual for the samples having low salinities,  
188 low temperatures and long freezing times, that the crack initiated and started to propagate along the bond and then  
189 slightly deviated and moved parallel to the bond but inside the parent material, as shown by Figure 5c.

#### 190 4. Discussion

191 The above results are the first measurements to be reported for the strength of freeze bonds under tensile  
192 loading. Although the experiments were performed under flexural loading, they provide unique data on the tensile  
193 strength of the freeze bonds. Under the loading conditions, the flexural strength of ice is governed by tensile strength  
194 ([assuming the material is linear-elastic and brittle](#)), although measured strengths are greater by a factor of about 1.7  
195 than strengths measured under pure tensile loading (Ashby and Jones, 2012). The reason is that in bending only a thin  
196 layer close to one surface of the sample (and thus a relatively small volume) carries the peak tensile stress and it is  
197 less likely that this volume contains larger flaw, while in tension the entire sample carries the tensile stress and it is  
198 more likely that it will contain larger flaws. Murdza et al. (2020b) showed that the flexural strength of freshwater S2  
199 ice tested on the same loading system as used here compares well with direct measurements of the tensile strength of  
200 the same type of ice at the same conditions (Carter, 1971) when divided by 1.7. Murdza et al. (2020b, 2021) showed  
201 that the flexural strength of lake Arctic ice tested under three-point bending is also similar to the the one obtained in  
202 Murdza et al. (2020b). By using this 1.7 factor to scale the values for saturated bond strengths shown in Figure 2 leads  
203 to tensile strength values of about 0.3 MPa and 0.18 MPa for bonds at -10 °C and -3 °C, respectively.  
204

205 While there are no other data on the tensile strength of freeze bonds, the results can be compared to the  
206 relatively large amount of earlier work on the shear strength of freeze bonds (Bailey et al., 2012; Boroojerdi et al.,  
207 2020a, 2020b; Bueide and Høyland, 2015; Ettema and Schaefer, 1986; Helgøy et al., 2013b, 2013a; Høyland and  
208 Møllegaard, 2014; Marchenko and Chenot, 2009; Repetto-Llamazares et al., 2011b, 2011a; Serré et al., 2011; Shafrova  
209 and Høyland, 2008; Szabo and Schneebeli, 2007). Common values for the shear strength in those studies ranged from  
210 0.01 to 0.1 MPa, which are considerably lower than the flexural strength values measured here. Usually, these  
211 strengths have been measured for bonds grown under water over periods that have not been long enough to reach  
212 saturated bond strengths. On the other hand, the highest reported shear strength values ~0.3...0.7 MPa (Bailey et al.,  
213 2012; Boroojerdi et al., 2020b; Shafrova and Høyland, 2008) are within the same range as the flexural strength values  
214 measured here. Given that the tensile strength of ice is, on average, lower than the shear strength (Timco and Weeks,  
215 2010), the strength values measured here are perhaps surprisingly high. The high strength values here likely relate to  
216 the well-controlled bond growing procedure and possibly to a finer microstructure of the material that comprises the  
217 bond.

218  
219 Work on the shear strength of freeze bonds has led to a conclusion that the evolution of the bond strength has  
220 three phases (Boroojerdi et al., 2020b; Repetto-Llamazares et al., 2011b, 2011a): (1) an initial period of a few minutes  
221 of increasing strength due to heat flux from the bond to the parent material; (2) a period of some hours of weakening  
222 as the temperature of the bond increases due to water surrounding it; and, (3) a period of several days of strengthening  
223 due to sintering. The evolution of the flexural strength of the bonds in the present experiments is likely similar to that  
224 of phases (1) and (3). The initial bond strengthening can be related to the transfer of heat along the long axis of the  
225 specimen and the accompanying advance of the ice/water interface. Given that the water layer after wetting the contact  
226 surfaces is very thin, the bond strength would be expected to saturate quickly; ~~Appendix B describes a simple model~~  
227 ~~and it is suggested~~ that the process, similar to above described phase (1), takes fewer than ~~10-30~~ minutes at -  
228 10 °C and a greater amount of time ~~of about 1.5 h~~ at -3 °C, aligning with earlier studies and the result here. This means  
229 that for saline bonds, phase (3) has a duration of about 6...12 hours, whereas earlier experiments have occasionally  
230 had relatively long freezing times, varying from 60 h to 12 days (Bailey et al., 2012; Shafrova and Høyland, 2008).

231  
232 As part of the studies on the evolution of bond strength, it has been fairly common to investigate the ratio of  
233 the bond strength values to that of the parent material (Bailey et al., 2012; Boroojerdi et al., 2020b; Shafrova and  
234 Høyland, 2008). Shafrova and Høyland (2008) found that specimens with bonds grown in the field had the strength  
235 ratio varying from 0.008 to 0.082 (with a mean of 0.03 after 48 hours of bonding). For laboratory-grown bonds, they  
236 measured ratios in the range 0.06 to 0.69 ( $0.21 \pm 0.12$ ). The latter values are in line with values reported by Bailey et  
237 al. (2011) and Boroojerdi et al. (2020b), who reported ratios up to about 0.70 and 0.85, respectively. Boroojerdi et al.  
238 (2020b) suggested an empirical formula to describe the strengthening of a freeze bond during the above-described  
239 phase (3). The formula was based on curve fitting and an assumption that the shear strength of the bond approaches  
240 asymptotically that of the parent material with increasing sintering time. The experiments here indicate that such an  
241 assumption may not be always justified, as at least the flexural strength of the freeze bonds can reach values that are

Formatted: Not Highlight

Formatted: Not Highlight

242 above that of the parent material. Aligning with our observations, the results by Høyland and Møllegaard (2014)  
243 provide an indication of the shear strength of freeze bonds reaching strengths comparable to that of the parent material.  
244 In their uniaxial compression tests on bonded cylindrical samples having an inclined freeze-bond, the failure changed  
245 from shearing (along the plane of the bond) to axial splitting of the sample in some of the cases.

246  
247 Ettema and Schaefer (1986) and Repetto-Llamazares et al. (2011b) studied whether freezing in the presence  
248 of water has an effect on the shear strength of the freeze-bond. The results indicate that shear strength was higher  
249 when bonds froze under water. While Ettema and Schaefer (1986) let the bonding occur with samples submerged in  
250 fresh water, Repetto-Llamazares et al. (2011b) used 7 ppt saline water for submerging. Earlier studies on the effect of  
251 freezing conditions have not had the opposing surfaces wetted before bringing them together when generating bonds  
252 in air. This effectively removes the above-described phase (1) from the bond strength evolution, if the result of the  
253 heat transfer during the initial period of bond strengthening is assumed to simply be freezing of the liquid at the bond  
254 interface. In addition, in these earlier studies, the maximum freezing times for the bonds grown in air varied only  
255 from 0.5 min to 3 min. As phase (3) takes at least several hours, it seems likely that the mentioned studies have not  
256 yielded data on saturated bond strengths for bonds grown in air.

257  
258 While the new data from the present tests yielded clear trends for the strength of the freeze-bonds, they also  
259 showed significant scatter. This scatter, even when bond generation was performed in a simplified manner using  
260 carefully prepared milled samples (Section 2), is an indication that the strength of freeze bonds is a parameter that  
261 inherently shows wide scatter. One reason for this, amongst others perhaps, is the detailed microstructure/phase  
262 distribution of the bond. The microstructure probably varies somewhat from specimen to specimen, thereby leading  
263 to variations in bond strength. The variation is actually of similar magnitude to that observed in experiments on the  
264 flexural strength of pristine ice samples made with the same apparatus (Murda et al., 2020c). The other reason,  
265 perhaps, can be attributed to the fact that a small volume of material is tested in bending and, hence, the variation in  
266 tensile strength if measured using a traditional methodology would likely be smaller, given the correlation coefficient  
267 between tensile and flexural strength is 1.7.

268  
269 The fact that in samples with freshwater bonds failure initiated and propagated outside of the bond suggests  
270 that the strength of the freshwater bond is greater than the strength of pristine freshwater S2 ice. This may indicate a  
271 difference in microstructure between the ice in the freeze bond and the ice of the parent plates. A finer grain size  
272 within the bonds may be due to the initial water layer, which was produced by spraying a very fine mist, creating small  
273 water droplets working as nucleation sites for the ice grains in the bond. Our argument is supported by the work of  
274 Schulson and others (1984) who showed that tensile strength strongly depends on the grain size, increasing as grain  
275 size decreases. A difference in grain size could also explain the fact that the strength versus salinity curve from Timco  
276 and O'Brien (1994) is below the trend obtained in the present study (Figure 3). Concerning of the microstructure of  
277 the bonds, one may think that because one phase is dominant it should form the matrix; however, there is at least one  
278 class of materials, namely high-temperature nickel-based superalloys (Sims, 1984) where the minor component forms



279 the matrix. Since we do not know the structure of the bonds in the present study, we cannot be conclusive in this  
280 regard.

281  
282 As expected, both temperature and salinity affect the flexural strength of bonded ice samples. The strength  
283 of both freshwater and saline ice increases over time and saturates, although saturation occurs significantly slower in  
284 the case of saline bonds. The reason is likely related to the rejected salts and entrapped air at the ice-water interface  
285 that slows the rate of the interface advance. The trend of saturated strength versus salinity (Figure 3) has an exponential  
286 functionality similar to what has been suggested by Timco and O'Brien (1994), while the trend of saturated strength  
287 versus temperature for saline bonds (Figure 4) appears, to a first approximation, to be roughly linear. It is important  
288 to mention here that the salinities provided in this paper are salinities of the spray and not of melt-water from the bond  
289 itself, and this begs the question: Is the bond salinity the same or lower than the salinity of spray solution? In the  
290 formation of a natural floating sea ice cover, of course, the rejection of salts from ice results in melt-water salinities  
291 lower than bulk water salinity (Weeks and Ackley, 1986). Given that in our experiments the bond thickness is very  
292 small (<1 mm) and freezing time is relatively short, it is unlikely that all the salt is expelled from the freeze bond,  
293 resulting in the bond salinity similar to the spray salinity. Therefore, while the resulting bonds might have salinities  
294 slightly lower than the sprayed water, the results yield a reasonably reliable trend of strength as a function of salinity  
295 which is very similar to the relationship proposed by Timco and O'Brien (1994).

296  
297 The effect of surface roughness at the freezing interface was also briefly addressed when performing the  
298 experiments. In addition to the milled surfaces with a roughness of  $0.43 \pm 0.24 \times 10^{-6}$  m in the direction of milling and  
299  $2.01 \pm 0.47 \times 10^{-6}$  m in the orthogonal direction (Schulson and Fortt, 2012), experiments were performed on samples  
300 with surfaces produced by using a fine and coarse band saw blade, which resulted in ice surface roughness of up to  
301 ~1 mm. The results from the experiments with differently produced surfaces showed no significant difference on the  
302 strength of freshwater and saline bonds (1.39 MPa vs  $1.43 \pm 0.15$  MPa for freshwater bonds and  $0.39 \pm 0.13$  MPa vs  
303  $0.34 \pm 0.16$  MPa for saline bonds of 12 ppt salinity). As milling could be performed with the highest accuracy from the  
304 aspect of sample dimensions and alignment, it was chosen as the technique we used here. Unlike what was observed  
305 in the present study, Helgøy et al. (2013a) observed that the surface roughness does affect freeze bond shear strengths,  
306 with rougher surface leading to bonds having higher strength. The discrepancy between their results and results in the  
307 present study suggests that there may exist a threshold value for the surface roughness, after which it affects the bond  
308 strength; it is likely that both milled and sawn surfaces used in the present study are too smooth for the effect of surface  
309 roughness to be observed. On the other hand, experiments on shear strength usually involve sliding motion between  
310 the blocks of the parent material. This motion may become restricted by rough surfaces, which could lead to higher  
311 shear loads interpreted to be due to an increase in freeze-bond strength. In tests under tensile loading, such kinematic  
312 restrictions do not exist.

313

314 Finally, it is worth noting that while this is the first study on the flexural strength of freeze bonds, it is not  
315 the complete story. Further work is needed to investigate the effects of other factors such as bond pressure, the  
316 character of parent ice plate, bond microstructure, the width of the opening to be bonded, etc.

## 317 **5. Conclusions**

318 Systematic experiments on the flexural strength of freeze bonds were conducted for the first time. The bonds  
319 were grown in the air under 4 kPa confining pressure. The parent material was S2 columnar-grained freshwater ice.  
320 The salinity of the bond varied from 0 to 35 ppt and freezing temperatures from -3 to -25 °C. It is concluded that:

- 321 (i) Freshwater bond strength exceeds the strength of parent ice in less than 0.5 h upon freezing.
- 322 (ii) The saline bonds reach their saturated strength within about 6-12 h of freezing.
- 323 (iii) An increase in bond salinity and in freezing temperature leads to a decrease in bond strength.
- 324 (iv) The relationship between bond strength and its salinity is similar to the one suggested by Timco and O'Brien  
325 (1994).
- 326 (v) No freezing occurs once the salinity of the water used to generate the bond reaches values of about ~25 ppt  
327 at -3 °C.

## 328 **Acknowledgements**

329 The authors are grateful for the financial support from the Academy of Finland through the project no. 309830 ("Ice  
330 Block Breakage: Experiments and Simulations (ICEBES)") and National Science Foundation (FAIN 1947-107). Arttu  
331 Polojärvi worked on the article while visiting Thayer School of Engineering at Dartmouth College (Hanover, NH,  
332 USA) during spring 2020, thanks are extended to Prof. Erland Schulson for hosting. Finnish Maritime Foundation is  
333 acknowledged for partial funding of the visit.

334  
335 **Author contributions:** AM, AP, ES, and CR designed the experiments, and AM carried them out. AM and AP  
336 prepared the manuscript with contributions from all co-authors.

337

338 **Competing interests:** The authors declare that they have no conflict of interest.

## 339 **References**

- 340 Arduin, F., Otero, M., Merrifield, S., Grouazel, A. and Terrill, E.: Ice Breakup Controls Dissipation of Wind Waves  
341 Across Southern Ocean Sea Ice, *Geophys. Res. Lett.*, 47(13), doi:10.1029/2020GL087699, 2020.
- 342 Ashby, M. M. and Jones, D. R. H.: *Engineering Materials 1: An Introduction to Properties, Applications and Design*,  
343 4th ed., Elsevier/Butterworth-Heinemann, Oxford, UK., 2012.

344 Asplin, M. G., Galley, R., Barber, D. G. and Prinsenberg, S.: Fracture of summer perennial sea ice by ocean swell as  
345 a result of Arctic storms, *J. Geophys. Res. Ocean.*, 117(6), 1–12, doi:10.1029/2011JC007221, 2012.

346 Bailey, E., Sammonds, P. R. and Feltham, D. L.: The consolidation and bond strength of rafted sea ice, *Cold Reg. Sci.*  
347 *Technol.*, 83–84, 37–48, doi:10.1016/j.coldregions.2012.06.002, 2012.

348 Boroojerdi, M. T., Bailey, E. and Taylor, R.: Experimental investigation of rate dependency of freeze bond strength,  
349 *Cold Reg. Sci. Technol.*, 178, 1–12, doi:10.1016/j.coldregions.2020.103120, 2020a.

350 Boroojerdi, M. T., Bailey, E. and Taylor, R.: Experimental study of the effect of submersion time on the strength  
351 development of freeze bonds, *Cold Reg. Sci. Technol.*, 172, 1–16, doi:10.1016/j.coldregions.2019.102986, 2020b.

352 Bueide, I. M. and Høyland, K. V.: Confined compression tests on saline and fresh freeze-bonds, in *Proceedings of the*  
353 *23rd International Conference on Port and Ocean Engineering under Arctic Conditions*, Trondheim, Norway., 2015.

354 Carter, D.: *Lois et mechanisms de l'apparente fracture fragile de la glace de riviere et de lac*, PhD Thesis, University  
355 of Laval., 1971.

356 Collins, C. O., Rogers, W. E., Marchenko, A. and Babanin, A. V.: In situ measurements of an energetic wave event  
357 in the Arctic marginal ice zone, *Geophys. Res. Lett.*, 42(6), 1863–1870, doi:10.1002/2015GL063063, 2015.

358 Ettema, R. and Schaefer, J. A.: Experiments on Freeze-Bonding Between Ice Blocks in Floating Ice rubble, *J. Glaciol.*,  
359 32(112), 397–403, doi:10.3189/S0022143000012107, 1986.

360 Ettema, R. and Urroz, G. E.: On internal friction and cohesion in unconsolidated ice rubble, *Cold Reg. Sci. Technol.*,  
361 16(3), 237–247, doi:10.1016/0165-232X(89)90025-6, 1989.

362 Frankenstein, G. and Garner, R.: Equations for Determining the Brine Volume of Sea Ice from  $-0.5^{\circ}$  to  $-22.9^{\circ}\text{C}$ ., *J.*  
363 *Glaciol.*, 6(48), 943–944, doi:10.3189/S0022143000020244, 1967.

364 Golding, N., Schulson, E. M. and Renshaw, C. E.: Shear faulting and localized heating in ice: The influence of  
365 confinement, *Acta Mater.*, 58, 5043–5056, doi:10.1016/j.actamat.2010.05.040, 2010.

366 Golding, N., Snyder, S. A., Schulson, E. M. and Renshaw, C. E.: Plastic faulting in saltwater ice, *J. Glaciol.*, 60(221),  
367 447–452, doi:10.3189/2014JoG13J178, 2014.

368 Heinonen, J.: *Constitutive modeling of ice rubble in first-year ridge keel*, Aalto University., 2004.

369 Helgøy, H., Astrup, O. S. and Høyland, K. V.: Laboratory work on freeze-bonds in ice rubble, Part I: Experimental  
370 set-up, Ice-properties and freeze-bond texture, in *Proceedings of the 22nd International Conference on Port and Ocean*  
371 *Engineering under Arctic Conditions*, Espoo, Finland., 2013a.

372 Helgøy, H., Astrup, O. S. and Høyland, K. V.: Laboratory work on freeze-bonds in ice rubble, Part II – Results from  
373 individual freeze bond experiments, in *Proceedings of the 22nd International Conference on Port and Ocean*  
374 *Engineering under Arctic Conditions*, Espoo, Finland., 2013b.

375 Høyland, K. V. and Møllegaard, A.: Mechanical behaviour of laboratory made freeze-bonds as a function of  
376 submersion time, initial ice temperature and sample size, in *22nd IAHR International Symposium on Ice*, pp. 265–  
377 273, Singapore., 2014.

378 Hwang, B., Wilkinson, J., Maksym, E., Graber, H. C., Schweiger, A., Horvat, C., Perovich, D. K., Arntsen, A. E.,  
379 Stanton, T. P., Ren, J. and Wadhams, P.: Winter-to-summer transition of Arctic sea ice breakup and floe size  
380 distribution in the Beaufort Sea, *Elem Sci Anth*, 5, 40, doi:10.1525/elementa.232, 2017.

381 Iliescu, D., Murdza, A., Schulson, E. M. and Renshaw, C. E.: Strengthening ice through cyclic loading, *J. Glaciol.*,  
382 63(240), 663–669, doi:10.1017/jog.2017.32, 2017.

383 Kohout, A. L., Williams, M. J. M., Dean, S. M. and Meylan, M. H.: Storm-induced sea-ice breakup and the  
384 implications for ice extent, *Nature*, 509(7502), 604–607, doi:10.1038/nature13262, 2014.

385 Kohout, A. L., Williams, M. J. M., Toyota, T., Lieser, J. and Hutchings, J.: In situ observations of wave-induced sea  
386 ice breakup, *Deep. Res. Part II Top. Stud. Oceanogr.*, 131, 22–27, doi:10.1016/j.dsr2.2015.06.010, 2016.

387 Liferov, P., Jensen, A. and Høyland, K. V.: On analysis of punch tests on ice rubble, in *Proceedings of the 16th*  
388 *International Symposium on Ice*, volume 2, pp. 101–110, Dunedin, New Zealand., 2002.

389 Liferov, P., Jensen, A. and Høyland, K. V.: 3D finite element analysis of laboratory punch tests on ice rubble, in  
390 *Proceedings of the 17th International Conference on Port and Ocean Engineering under Arctic Conditions, POAC'03*,  
391 volume 2, pp. 611–621, Trondheim, Norway., 2003.

392 Marchenko, A. and Chenot, C.: Regelation of ice blocks in the water and on the air, in *Proceedings of the 20th*  
393 *International Conference on Port and Ocean Engineering under Arctic Conditions*, Luleå, Sweden., 2009.

394 Michel, B. and Ramseier, R. O.: Classification of river and lake ice, *Can. Geotech. J.*, 8(1), 36–45, doi:10.1139/t71-  
395 004, 1971.

396 Murdza, A., Schulson, E. M. and Renshaw, C. E.: Hysteretic behavior of freshwater ice under cyclic loading :  
397 preliminary results, in *24th IAHR International Symposium on Ice*, pp. 185–192, Vladivostok., 2018.

398 Murdza, A., Schulson, E. M. and Renshaw, C. E.: The effect of cyclic loading on the flexural strength of columnar  
399 freshwater ice, in *Proceedings of the International Conference on Port and Ocean Engineering under Arctic*  
400 *Conditions, POAC*, vol. 2019-June., 2019.

401 Murdza, A., Schulson, E. and Renshaw, C.: Behavior of Saline Ice under Cyclic Flexural Loading, *Cryosph. Discuss.*,  
402 1–22, doi:10.5194/tc-2020-300, in press, 2020a.

403 Murdza, A., Marchenko, A., Schulson, E., Renshaw, C., Sakharov, A., Karulin, E. and Chistyakov, P.: Results of  
404 preliminary cyclic loading experiments on natural lake ice and sea ice, in *25th IAHR International Symposium on Ice*,  
405 pp. 1–10, Trondheim, Norway., 2020b.

406 Murdza, A., Schulson, E. M. and Renshaw, C. E.: Strengthening of columnar-grained freshwater ice through cyclic  
407 flexural loading, *J. Glaciol.*, 66(258), 556–566, doi:10.1017/jog.2020.31, 2020c.

408 Murdza, A., Marchenko, A., Schulson, E. M. and Renshaw, C. E.: Cyclic strengthening of lake ice, *J. Glaciol.*, 67(261),  
409 182–185, doi:10.1017/jog.2020.86, 2021.

410 Polojärvi, A. and Tuhkuri, J.: On modeling cohesive ridge keel punch through tests with a combined finite-discrete  
411 element method, *Cold Reg. Sci. Technol.*, 85, 191–205, doi:10.1016/j.coldregions.2012.09.013, 2013.

412 Repetto-Llamazares, A. H. V., Høyland, K. V. and Kim, E.: Experimental studies on shear failure of freeze-bonds in  
413 saline ice.: Part II: Ice-ice friction after failure and failure energy, *Cold Reg. Sci. Technol.*, 65(3), 298–307,  
414 doi:10.1016/j.coldregions.2010.12.002, 2011a.

415 Repetto-Llamazares, A. H. V., Høyland, K. V. and Evers, K. U.: Experimental studies on shear failure of freeze-bonds  
416 in saline ice: Part I. Set-up, failure mode and freeze-bond strength, *Cold Reg. Sci. Technol.*, 65(3), 286–297,  
417 doi:10.1016/j.coldregions.2010.12.001, 2011b.

418 Schulson, E. M. and Fortt, A. L.: Friction of ice on ice, *J. Geophys. Res. Solid Earth*, 117(B12), n/a-n/a,  
419 doi:10.1029/2012JB009219, 2012.

420 Schulson, E. M., Lim, P. N. and Lee, R. W.: A brittle to ductile transition in ice under tension, *Philos. Mag. A*, 49(3),  
421 353–363, doi:10.1080/01418618408233279, 1984.

422 Serré, N.: Mechanical properties of model ice ridge keels, *Cold Reg. Sci. Technol.*, 67(3), 89–106,  
423 doi:10.1016/j.coldregions.2011.02.007, 2011a.

424 Serré, N.: Numerical modelling of ice ridge keel action on subsea structures, *Cold Reg. Sci. Technol.*, 67(3), 107–119,  
425 doi:10.1016/j.coldregions.2011.02.011, 2011b.

426 Serré, N., Repetto-Llamazares, A. H. V. and Høyland, K.: Experiments on the relation between freezebond and ice  
427 rubble strength, part I: shear box experiments, in *Proceedings of the 21st International Conference on Port and Ocean  
428 Engineering under Arctic Conditions*, pp. 1–18, Montreal, Canada., 2011.

429 Shackleton, E. H.: *South: The Story of Shackleton's Last Expedition, 1914–17*, Macmillan, USA., 1982.

430 Shafrova, S. and Høyland, K. V.: The freeze-bond strength in first-year ice ridges. Small-scale field and laboratory  
431 experiments, *Cold Reg. Sci. Technol.*, 54(1), 54–71, doi:10.1016/j.coldregions.2007.11.005, 2008.

432 Shen, H. H.: *Wave-Ice Interactions*, in *Encyclopedia of Maritime and Offshore Engineering*, John Wiley & Sons, Ltd,  
433 Chichester, UK., 2017.

434 Sims, C. T.: A History of Superalloy Metallurgy for Superalloy Metallurgists, in *Superalloys 1984 (Fifth International  
435 Symposium)*, pp. 399–419, The Minerals, Metals and Materials Society, Warrendale, PA., 1984.

436 Smith, T. R. and Schulson, E. M.: The brittle compressive failure of fresh-water columnar ice under biaxial loading,  
437 *Acta Metall. Mater.*, 41(1), 153–163, doi:10.1016/0956-7151(93)90347-U, 1993.

438 Snyder, S. A., Schulson, E. M. and Renshaw, C. E.: Effects of prestrain on the ductile-to-brittle transition of ice, *Acta  
439 Mater.*, 108, 110–127, doi:10.1016/j.actamat.2016.01.062, 2016.

440 Squire, V. A.: Ocean Wave Interactions with Sea Ice: A Reappraisal, *Annu. Rev. Fluid Mech.*, 52(1), 37–60,  
441 doi:10.1146/annurev-fluid-010719-060301, 2020.

442 Szabo, D. and Schneebeli, M.: Subsecond sintering of ice, *Appl. Phys. Lett.*, 90(151916), 1–3, doi:10.1063/1.2721391,  
443 2007.

444 Timco, G. W. and O'Brien, S.: Flexural strength equation for sea ice, *Cold Reg. Sci. Technol.*, 22(3), 285–298,  
445 doi:10.1016/0165-232X(94)90006-X, 1994.

446 Timco, G. W. and Weeks, W. F.: A review of the engineering properties of sea ice, *Cold Reg. Sci. Technol.*, 60(2),  
447 107–129, doi:10.1016/J.COLDREGIONS.2009.10.003, 2010.

448 Weeks, W. F. and Ackley, S. F.: The Growth, Structure, and Properties of Sea Ice, in *The Geophysics of Sea Ice*, pp.  
449 9–164, Springer US, Boston, MA., 1986.

450

451

452 **Appendix A. The relation between major and minor stresses in a sample in four-point bending**

453 ——— To find a relationship between major and minor principal stresses in the ice plate we consider two cases: the  
454 ice behaves as an isotropic linear elastic material and ice behaves as plastically isotropic material.

455 Stress tensor for the ice plate bent in a four-point manner ( $x1$  direction is along the long axis of the ice plate;  
456  $x2$  direction is along the width  $b$  of the specimen;  $x3$  direction is along the thickness of the ice plate):

$$\sigma_{ij} = \begin{pmatrix} \sigma_{11} & 0 & 0 \\ 0 & \sigma_{22} & 0 \\ 0 & 0 & 0 \end{pmatrix}.$$

459 Strain tensor for the ice plate bent in a 4-point manner:

$$\epsilon_{ij} = \begin{pmatrix} \epsilon_{11} & 0 & 0 \\ 0 & 0 & 0 \\ 0 & 0 & \epsilon_{33} \end{pmatrix}.$$

463 Incremental plastic strain tensor:

$$d\epsilon_{ij}^p = \begin{pmatrix} d\epsilon_{11}^p & 0 & 0 \\ 0 & 0 & 0 \\ 0 & 0 & d\epsilon_{33}^p \end{pmatrix}.$$

467 A constitutive relationship for isotropic linear elastic material (Hooke's law):

$$\epsilon_{22} = \frac{1}{E} [\sigma_{22} - \nu(\sigma_{11} + \sigma_{33})];$$

$$\sigma_{22} = \nu\sigma_{11} = \frac{1}{3}\sigma_{11}.$$

474 A constitutive relationship for plastically isotropic material beyond yielding (Levy-Mises Flow Rule):

$$d\epsilon_{22}^p = \frac{d\bar{\epsilon}^p}{\bar{\sigma}} \left[ \sigma_{22} - \frac{1}{2}(\sigma_{11} + \sigma_{33}) \right];$$

$$\sigma_{22} = \frac{1}{2}\sigma_{11}$$

480 where  $\bar{\sigma}$  is effective stress (also significant or equivalent stress);  $d\bar{\epsilon}^p$  is an effective plastic strain increment.

482 Hence, the minor stress  $\sigma_{zz}$  is approximately between one third to one half of the major stress  $\sigma_{xx}$ .

### 483 **Appendix B: Time for the freeze-bond formation**

484 To estimate the time to form a freeze bond we assume that heat fluxes are along the long axis of the sample,  
485 i.e. horizontal temperature gradients are much larger than vertical gradients at the freezing interface. The other  
486 assumptions are that the heat flow through a material is equal to the energy for the solidification of the water along  
487 the bond and that no heat losses occur, i.e.

$$488 \quad k \frac{dT}{dx} = \rho \lambda \frac{dx}{dt} \quad (A1)$$

489 where  $t$  is the time,  $T$  is the ice temperature,  $k$  is the thermal conductivity of ice,  $\lambda$  is the latent heat of fusion of ice  
490 per unit mass,  $\rho$  is the ice density and  $\Delta x$  is the characteristic conduction length or, in our case, the thickness of the  
491 bond.  
492

493 Taking into account that thermal diffusivity  $\alpha = k/\rho c_p$ , where  $c_p$  is specific heat capacity, and that  $x = \sqrt{\alpha t}$ ,  
494 after integration of Equation A1, and further assuming time interval to be  $[0, t]$  and interval for the characteristic  
495 conduction length to be  $[0, x]$ , we obtain the relationship:

$$496 \quad t = \frac{1}{4} \left( \frac{x\lambda}{\Delta T} \right)^2 \left( \frac{\rho}{k c_p} \right) \quad (A2)$$

497 A note of caution is necessary here. As ice-water interface advances during freezing in saline ice, both air  
498 and salt are rejected and build up at the interface. Unlike freezing in nature, there is not enough space for rejection  
499 and, as a result, this slows the rate of advance of the interface.

500  
501 According to Equation A2, and using parametric values of  $c_p = 2100 \text{ J/kg}^\circ\text{C}$ ,  $\lambda = 330 \text{ kJ/kg}$ ,  $k =$   
502  $2.2 \text{ W/m}^\circ\text{C}$ ,  $\rho = 914 \text{ kg/m}^3$  for freshwater ice at  $-10^\circ\text{C}$  and bond thickness of 1 mm we need only 1 min for the  
503 bond formation, while for freshwater ice at  $-3^\circ\text{C}$  a similar bond forms in about 10 minutes. While this estimate is  
504 consistent with observations, it is also in accord with earlier experimental results by Repetto Llamazares et al. (2011a,  
505 2011b) and Borojeerdi et al. (2020a) for phase (1) increase during freeze-bond shear strength evolution (Section 4).

507

### 508 **Appendix CA: The strength of freeze-bonds as a function of salinity and temperature**

509 Principle:

510

511 The freeze bond is comprised of essentially two phases, solid (ice) plus liquid (water), barring entrapped air.  
 512 To a first approximation, we assume that its strength,  $\sigma_{fb}$ , is proportional to the volume fraction,  $f_s$ , of the solid phase.  
 513 The constant of proportionality,  $\sigma_{f0}$ , is the strength of freshwater ice. The relationship:

$$\sigma_{fb} = \sigma_{f0} f_s . \quad (\text{A3})$$

514 The volume fraction of the solid phase is obtained from the lever rule:

$$f_s = \frac{X_l - X_0}{X_l - X_s} , \quad (\text{A4})$$

515 where  $X_l$  and  $X_s$  denote the limit of solubility of salt in the liquid (water) and in the solid (ice) phases, respectively,  
 516 and  $X_0$  is the concentration of salt in the water before freezing is initiated. Over the temperature range of interest, the  
 517 phase diagram for the  $\text{H}_2\text{O}$ -NaCl system (i.e., thermodynamics) dictates that both  $X_l$  and  $X_s$  increases with decreasing  
 518 temperature,  $T$ , according to the relationships:

$$X_l = \frac{T - T_0}{m_l} , \quad (\text{A5})$$

$$X_s = \frac{T - T_0}{m_s} , \quad (\text{A6})$$

519 where  $T_0$  denotes the melting point of "pure" ice (273 K) and  $m_l$  and  $m_s$ , respectively, denote the slope of the liquidus  
 520 and the solidus on the phase diagram; both slopes are negative. The solubility of salt in ice is very low and so for  
 521 practical purposes  $X_s \sim 0$ . Writing the temperature difference as  $T - T_0 = \Delta T$ , the volume fraction of ice within the  
 522 freeze bond from Eqn (A4) is given by:

$$f_s = \left( 1 - \frac{m_l X_0}{\Delta T} \right) . \quad (\text{A7})$$

523 Thus, upon equating  $X_0$  to salinity,  $S$ , the strength of the freeze bond is given by:

$$\sigma_{fb} = \sigma_{f0} \left( 1 - \frac{m_l S}{\Delta T} \right) . \quad (\text{A8})$$

524 Taking  $m_l$  to be independent of concentration, its value is  $m_l = -0.1 \text{ K psu}^{-1}$ , giving:

$$\sigma_{fb} = \sigma_{f0} \left( 1 + \frac{0.1S}{\Delta T} \right) , \quad (\text{A9})$$

525 where  $\Delta T < 0$ .

526  
 527 The model thus dictates that once freezing is complete the strength of the freeze bond decreases linearly with  
 528 increasing salinity, reaching the limit of zero strength when  $S = \Delta T / -m_l$ .

529  
 530 Both dictates are in reasonable agreement with observation.

531  
 532 **Appendix DB: Trends in Figure 3**

533



534 The red trend in Figure 3 is taken from (Timco and O'Brien, 1994) where the authors report values for  
535 flexural strength of saline ice over the range of salinities used in the present study and for temperatures above -4.5°C  
536 ( $\sigma_f$  in MPa), i.e.

537

$$\sigma_f = 1.76e^{-5.88\sqrt{v_b}}. \quad (\text{A10})$$

538

539

540 To calculate salinity  $S$  (in ppt) based on the liquid brine content  $v_b$  (brine volume fraction) in Timco and  
541 O'Brien (1994) we used the following relationship suggested by (Frankenstein and Garner, 1967):

542

$$v_b = S \left( \frac{49.185}{|T|} + 0.532 \right) \quad (\text{A11})$$

543

544 where  $T$  is the ice temperature in degrees Celsius between -0.5 °C and -22.9 °C. The fit to our data in Figure 3 (black  
545 curve) was made according to the least square method which resulted in the following equation ( $\sigma_f$  in MPa):

546

$$\sigma_f = 1.12e^{-5.88v_b} \quad (\text{A12})$$

547

548

549

550

551

552

553

554

555

556

557

558

559

560

561

562

563

564

565

566

567  
568  
569

570 **Table 1. Results from testing freshwater bond experiments. The time here is the bond formation time, the strength is the**  
571 **flexural strength (temperature during flexural testing and bond formation was the same). The reader should notice that in**  
572 **all of these experiments the failure occurred outside of the bond and within the parent material.**

Sample #	Temperature [°C]	Time [h]	Strength [MPa]
1	-10	24	1.43
2	-10	25	1.39
3	-10	24	1.28
4	-10	3	1.58
5	-3	1.5	1.02
6	-3	1.5	1.28
7	-3	0.5	1.4

573  
574

**Table 2. Results from testing saline bond experiments at -10 °C and 35 ppt.**

Sample #	Time [h]	Strength [MPa]
8	1.5	0.15
9	3	0.1
10	26	0.34
11	34	0.54
12	25	0.64
13	82	0.61
14	6	0.38
15	12	0.54

575  
576

**Table 3. Results from testing saline bond experiments at -3 °C and 12 ppt.**

Sample #	Time [h]	Strength [MPa]
16	1.5	Low
17	1.5	0.31
18	3	0.17
19	3	0.18
20	6	0.25
21	6	0.22
22	14	0.48
23	24	0.14
24	24	0.35
25	72	0.29
26	97	0.32

577

578

579 **Table 4. Results from testing saline bond experiments at -3 °C.**

Sample #	Salinity [ppt]	Time [h]	Strength [MPa]
27	35	1.5	No*
28	35	24	No*
29	25	24	No*
30	20	28	0.12
31	17	3	Low*
32	17	13	Low*
33	17	25	0.3
34	17	113	0.28
35	10	24	0.34
36	10	24	0.34
37	10	24	0.41
38	10	26	0.77
39	10	73	0.54
40	5	21	0.37
41	5	24	0.46
42	5	24	0.75
43	2	25	0.62
44	2	24	0.91

580 \* "No" and "Low" correspond to "No freezing occurred" and "Strength was too small to be measured", respectively.

581

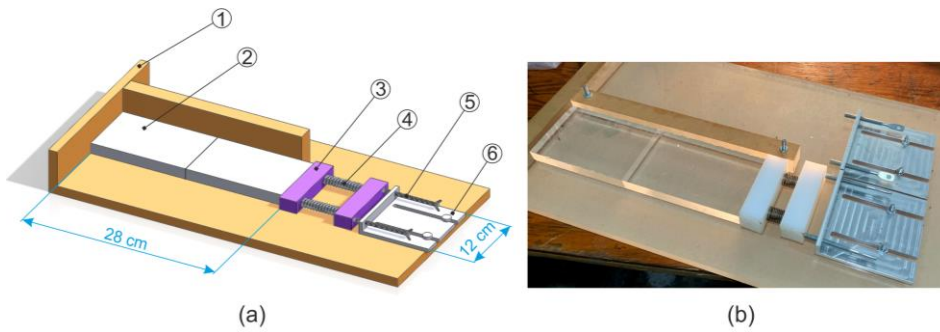
582 **Table 5. Results from testing of ice with bond salinity of 20 ppt after ~24 h of freezing.**

Sample #	Temperature [°C]	Strength [MPa]
45	-25	1.69*
46	-25	1.67*
47	-25	1.47*
48	-25	1.13
49	-20	1.25
50	-20	0.71
51	-15	0.87
52	-15	0.76
53	-15	0.63
54	-15	0.55
55	-15	0.35
56	-15	0.2
57	-10	0.66
58	-10	0.64

Sample #	Temperature [°C]	Strength [MPa]
59	-10	0.46
60	-10	0.4
61	-5	0.2
62	-5	0.1
63	-3	0.12

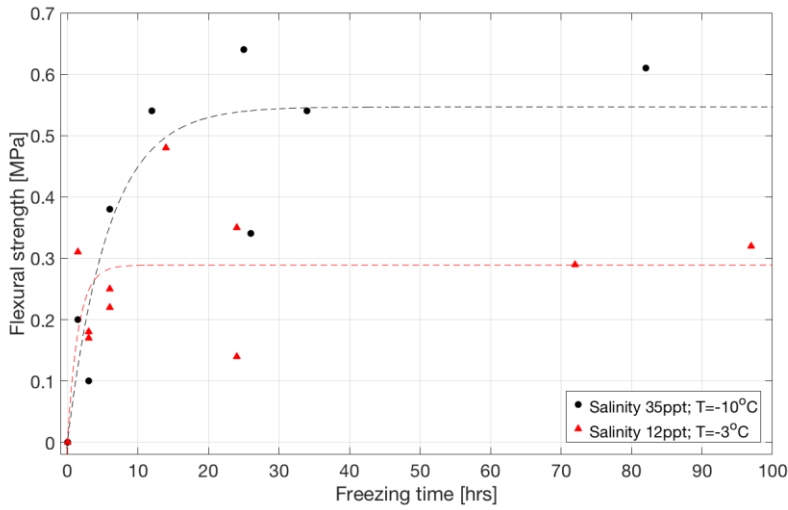
\*failure occurred outside the bond.

583  
584  
585  
586

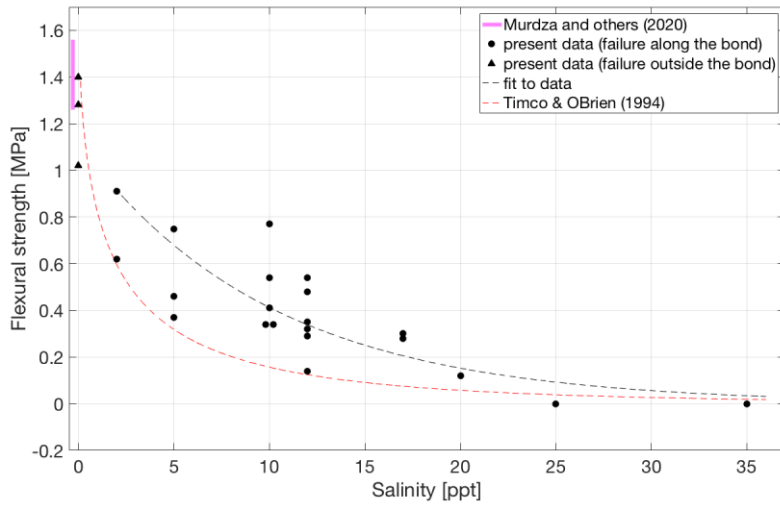


587  
588  
589

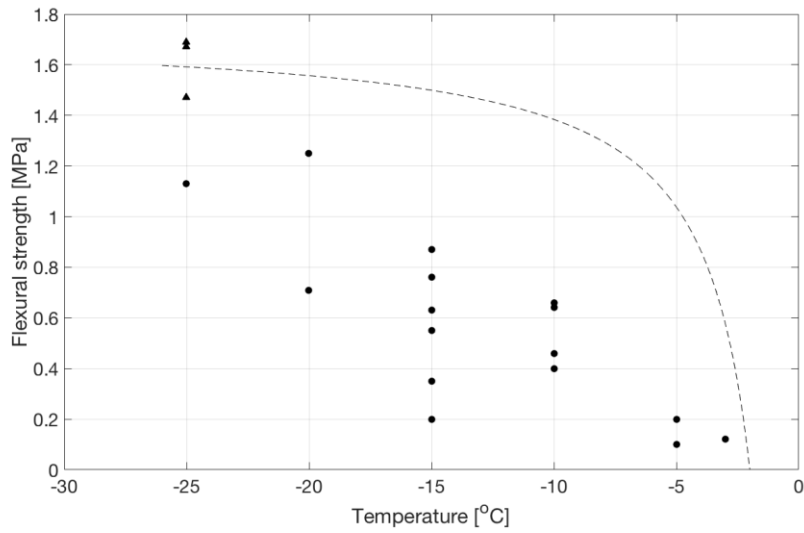
Figure 1. Sketch (a) and photograph (b) of the freeze-bonding rig with an ice sample having the shape of a thin plate: 1 – acrylic plate; 2 – ice specimen; 3 – plastic bar; 4 – spring; 5 – bolt; 6 – fixation plate.



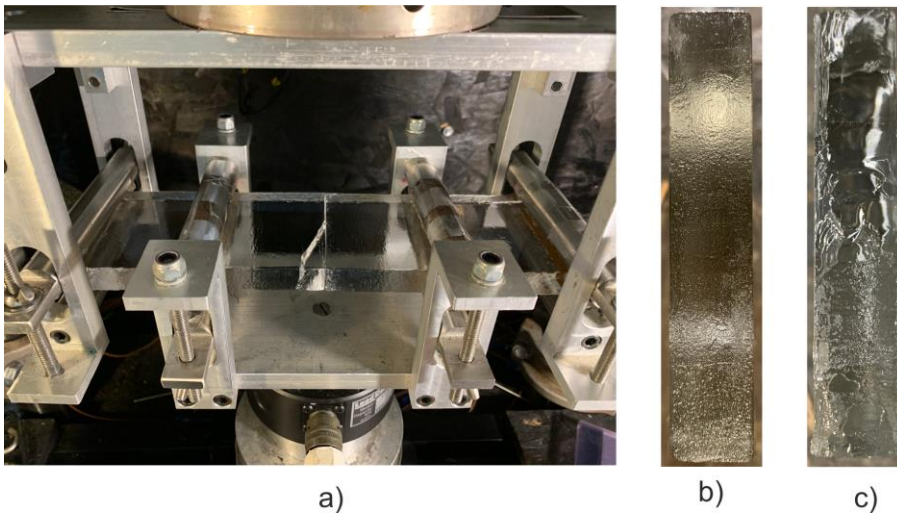
590  
 591 **Figure 2. Flexural strength as a function of freezing time for bonded ice prepared from salt water of 35 ppt salinity at -10°C**  
 592 **(in black) and from salt water of 12 ppt salinity at -3°C (in red).**



593  
 594 **Figure 3. Flexural strength at -3 °C of bonded ice as a function of the salinity of the salt water from which the bond was**  
 595 **formed. The solid pink line indicates the flexural strength 1.42±0.16 MPa of parent freshwater ice at -3 °C (Murdza et al.,**  
 596 **2020c). A red dashed line is taken from Timco and O'Brien (1994) for the ice at -3 °C. A black dashed line is a fit to the**  
 597 **present data.**



598  
 599 **Figure 4. Flexural strength of bonded ice as a function of temperature for bonds formed from water of salinity of 20 ppt.**  
 600 **Triangular-shaped points at -25 °C indicate that actual bond strength is greater than that of the parent material as the**  
 601 **failure occurred outside the bond. The dotted line is drawn according to the model in Appendix [EA](#).**



602  
 603 **Figure 5. Photographs of an ice sample #38 right after forced failure (a); the saline bond surface of 10 ppt after a crack**  
 604 **propagated fully through the bond, sample #19 (b) and partially through the parent material, sample #47 (c).**

605